Letters

Dual-Mode Bidirectional *LLC*-DAB Converter Based on a Modulated Coupled Inductor

Xiaoying Chen, *Graduate Student Member, IEEE*, Guo Xu, *Senior Member, IEEE*, Hua Han, *Member, IEEE*, Yao Sun, *Member, IEEE*, and Mei Su, *Member, IEEE*

***Abstract*—The *LLC* resonant converter and dual-active-bridge (DAB) converter are attractive topologies to be used in bidirectional power applications for their respective advantages. In this letter, a dual-mode bidirectional *LLC*-DAB converter based on a modulated coupled inductor is proposed to combine the *LLC* and DAB converter into a single converter. By only modulating the PWM signals, the *LC* tank of the converter in two operation modes can be changed without adding any other additional diodes or switches. Meanwhile, by utilizing the modulated coupled inductor, the inductance of the *LC* tank will be different for two operation modes. The small leakage inductance is suitable for resonance with resonant capacitor in the *LLC* mode. And the large inductance is adopted to transfer the power in the DAB mode. Therefore, the *LC* tank parameters for two operation modes can be designed separately. The principle of the proposed dual-mode converter based on the modulated coupled inductor is investigated. After that, the parameters design consideration of the converter is given. Finally, a 2000-W prototype is built to verify the effectiveness of the proposed converter.**

***Index Terms*—Bidirectional DC– converter, dual active bridge (DAB), *LLC*.**

I. Introduction

With the rapid development of the renewable power system, dc distribution systems, electric vehicles, power storage systems, and so on, an efficient isolation bidirectional dc– converter (IBDC) becomes a critical unit for handling the bidirectional power flow [1]. For the topology of the IBDC, the *LLC* converter and the dual-active-bridge (DAB) converter are attractive solutions for the advantage of high efficiency, high power density, soft-switching, and easy implementation [2].

Manuscript received 6 June 2022; revised 25 July 2022; accepted 2 September 2022. Date of publication 6 September 2022; date of current version 10 October 2022. This work was supported in part by the State Key Laboratory of Power System and Generation Equipment under Grant SKLD21KM06, in part by the National Science Foundation of China under Grant 51907206, Grant 61933011, and Grant 62192754, and in part by the Fundamental Research Funds in the Central South University under Grant 2021zzts0187. *(Corresponding author: Guo Xu.)*

The authors are with the Hunan Provincial Key Laboratory of Power Electronics Equipment and Grid, School of Automation, Central South University, Changsha 410083, China (e-mail: chenxiaoying01@csu.edu.cn; xuguocsu@csu.edu.cn; hua_han@126.com; yaosuncsu@gmail.com; sumeicsu@csu.edu.cn).

Color versions of one or more figures in this article are available at https://doi.org/10.1109/TPEL.2022.3204529.

Digital Object Identifier 10.1109/TPEL.2022.3204529

The topology of the bidirectional *LLC* and DAB converter is similar, which contains two full-bridge or half-bridge and an *LC* tank. For *LLC* converters, the primary switches act as an inverter, and the secondary switches are driven synchronously [3]. Besides, when the converter operates in the bidirectional application, the driving logic needs to be exchanged [4]. On the other hand, for the DAB converters, all switches are driven actively [5]. Besides, the converter can achieve natural bidirectional power flow by applying the phase-shift control strategy [6]. The major difference between *LLC* and DAB converters is the *LC* tank. For an *LLC* converter, the resonant frequency of the *LC* tank is designed around the switching frequency. And the impedance of the *LC* tank is small. However, for the DAB converter, the capacitor of the *LC* tank is used for dc blocking, even without the dc blocking capacitor. And the impedance of the *LC* tank is inductive. Besides, the inductance of the *LC* tank in the *LLC* converter is relatively smaller than that in the DAB converter.

Comparing two converters, both have their respective advantages [7]. Therefore, many researchers try to modify the topology to combine the advantages of both *LLC* converter and DAB converter [8], [9], [10], [11]. One method to combine *LLC* and DAB converters is to connect two kinds of converters with modular structures or multiport structures. To combine the efficiency advantage of the *LLC* converter and the controllability of the DAB converter, a hybrid converter was proposed in [8]. The *LLC* converters process the majority part of the power, and the DAB converter is responsible for flexible control. A three-port dc/dc converter based on the series resonant converter and DAB converter for the hybrid charging station is proposed in [9]. The fast-charging port is based on series resonant converter with unidirectional power flow. And slow-charging port based on the DAB converter handles the bidirectional power flow. However, by using the modular structure or multiport structure, the number of switches will increase.

Another method to combine *LLC* and DAB converters is to change the *LC* tank structure for a single converter. To solve the start-up and overload protection issues of the resonant converter, an isolated dc/dc bus converter combining the resonant converter and DAB converter was proposed in [10]. By bypassing the resonant capacitor, the converter can work under the DAB mixed mode to avoid overload. With a similar working principle,

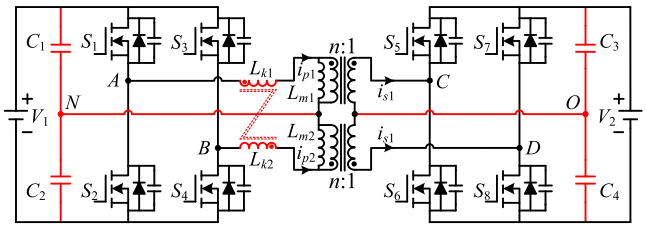

Fig. 1. Proposed dual-mode bidirectional *LLC*-DAB converter.

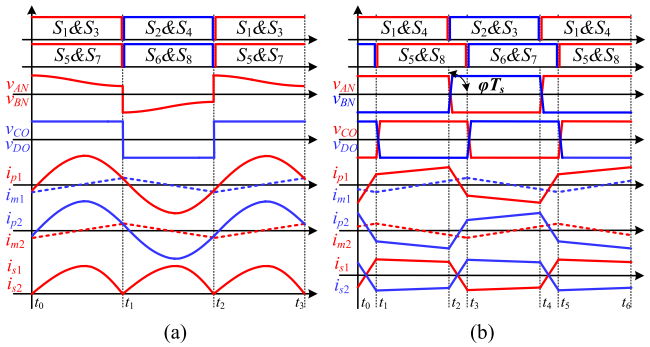

Fig. 2. Key operation waveforms of the proposed converter. (a) *LLC* mode. (b) DAB mode.

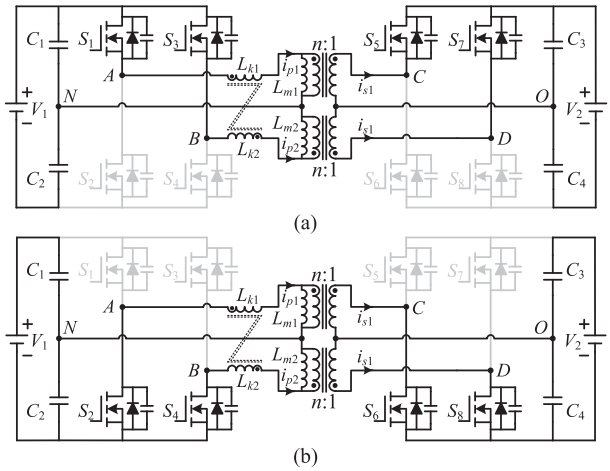

Fig. 3. Equivalent circuit of the converter in the *LLC* mode. (a) During $t_0 \sim t_1$. (b) During $t_1 \sim t_2$.

the capacitor-clamped *LLC* converter was proposed to achieve overcurrent protection and reduce the flux linkage requirement in transformers for electric vehicles [11]. However, for the converter in [10] and [11], the power flow is unidirectional, and the diode-based rectifier may not be suitable for large output current applications. A tunable immittance-based DAB converter was proposed in [12] to achieve zero backflow power and ZVS for all switches by adding a tunable resonant network for the DAB converter. While, similar to [10] and [11], the auxiliary diodes or switches need to be added to change the *LC* tank structure in [12], which will increase the complexity of the converter. In [13], a concept of a modulated coupled inductor is proposed by the authors of this letter, and by modulating the PWM signals, the *LC* tank parameters of the DAB converter will be changeable. However, this method cannot change the *LC* tank structure and is only used to limit the start-up current and reduce the rms current in steady state.

In this letter, a dual-mode bidirectional *LLC*-DAB converter is proposed to combine the *LLC* and DAB converter. The converter can exchange the operation modes of *LLC* and DAB by changing the *LC* tank structure, which can be changed by modulating the PWM signals without adding any other additional auxiliary diodes or switches. Meanwhile, by utilizing the modulated coupled inductor, the equivalent inductance can be different for two operation modes. The small inductance is suitable for resonance with resonant capacitors in the *LLC* mode. And the large inductance is adopted to transfer the power in the DAB mode. Therefore, the *LC* tank parameters can be designed separately for the two operation modes.

II. Principle of the Proposed Dual-Mode *LLC*-DAB Converter

A. Circuit of the Proposed Dual-Mode Converter

The schematic circuit of the proposed converter is illustrated in Fig. 1. As seen, the proposed converter is modified based on the conventional DAB converter. To achieve the small equivalent inductance resonating with the resonant capacitor in the *LLC* mode and the large equivalent inductance transferring power flow in the DAB mode, the leakage inductors L_{k1} and L_{k2} are negatively coupled to be used as a modulated coupled inductor, which can change the equivalent inductance by modulating the PWM signals. The middle nodes *N* and *O* of the split capacitors (C_1 and C_2, C_3 and C_4) are connected to the middle nodes of two split transformers. C_1 and C_2 are acted as resonant capacitors. For symmetry of the converter, $C_1 = C_2$, $C_3 = C_4$, $L_{k1} = L_{k2} = L_k$, and $L_{m1} = L_{m2} = L_m$. The turns ratio n of the two transformers is the same.

B. Working Principle of the Proposed Converter

The proposed converter can be switched between *LLC* and DAB modes through changing the switch driving pattern, whose working waveforms are illustrated in Fig. 2. As seen, when the converter operates in the *LLC* mode, the driving signals of S_1 and S_3 are the same, and the driving signals of S_5 and S_7 are the same. While the converter operates in the DAB mode, the driving signals of S_1 and S_4 are the same, and the driving signals of S_5 and S_8 are the same. Meanwhile, the phase between the driving signals of S_1 and S_5 is modulated to control the transferred power.

1) LLC *Mode:* When the converter operates in the *LLC* mode, the key waveforms and the equivalent circuit are shown in Figs. 2(a) and 3, respectively. As seen, the driving signals of S_1 and S_3 are the same, and S_5 and S_7 are the same. And the converter can be regarded as two parallel-connected half-bridge *LLC* converters in this mode. As shown in Fig. 3(a), when S_1 and S_3 are turned ON, v_{AN} and v_{BN} are equal to the voltage across the resonant capacitor C_1, which can be expressed as $v_{AN} = v_{BN} = v_{C1}$. Meanwhile, v_{CO} and v_{DO} are equal to the voltage

across the split capacitor C_3, which can be expressed as $v_{CO} = v_{DO} = v_{C3}$. As shown in Fig. 3(b), when S_2 and S_4 are turned ON, v_{AN} and v_{BN} are opposite to the voltage across the resonant capacitor C_2, which can be expressed as $v_{AN} = v_{BN} = -v_{C2}$. Meanwhile, v_{CO} and v_{DO} are opposite to the voltage across the split capacitor C_4, which can be expressed as $v_{CO} = v_{DO} =$ -v_{C4}.

In this mode, because $v_{AN} = v_{BN}$, $v_{CO} = v_{DO}$, the direction of i_{p1} and i_{p2} will be the same. Then, the current flow into node *N* is ($i_{p1} + i_{p2}$). The current flow into node *O* is ($i_{s1} + i_{s2}$). Meanwhile, C_1, C_2, L_{k1}, and L_{k2} form an *LC* resonant tank.

For the negatively coupled inductor in the proposed converter, its mathematical model can be expressed as

$$\begin{cases} v_{L1} = L_{k1}\frac{di_{p1}}{dt} - M\frac{di_{p2}}{dt} \\ v_{L2} = L_{k2}\frac{di_{p2}}{dt} - M\frac{di_{p1}}{dt} \end{cases} \tag{1}$$

where v_{L1} and v_{L2} are the voltages across the two windings of the coupled inductor, respectively. L_{k1} and L_{k2} are the self-inductance, and *M* is the mutual inductance. Because of the symmetry of the converter, $L_{k1} = L_{k2} = L_k$. In this mode, the amplitude and the direction of i_{p1} and i_{p2} are the same, namely $i_{p1} = i_{p2}$. Then, (1) can be rearranged as

$$\begin{cases} v_{L1} = (L_k - M)\frac{di_{p1}}{dt} \\ v_{L2} = (L_k - M)\frac{di_{p1}}{dt} \end{cases}. \tag{2}$$

According to the current–voltage relationship of the inductor, it can be obtained from (2) that the equivalent inductance of the modulated coupled inductor in the *LLC* mode is

$$L_{LLC} = (L_k - M) = (1 - k)L_k \tag{3}$$

where *k* is the coupling coefficient of the coupled inductor, which is defined as $k = M/L_k$.

The resonant frequency f_r of the converter is expressed as

$$f_r = \frac{1}{2\pi\sqrt{L_{LLC}C_1}} = \frac{1}{2\pi\sqrt{(1-k)L_kC_1}}. \tag{4}$$

2) DAB Mode: When the converter operates in the DAB mode, the working waveforms and the equivalent circuit are shown in Figs. 2(b) and 4, respectively. As seen, the driving signals of S_1 and S_4 are the same. S_5 and S_8 are the same. In this mode, the split capacitors C_1∼C_4 will be bypassed, and the converter can operate as a full-bridge DAB converter. And the phase-shift ratio between v_{AB} and v_{CD} is defined as φ. As shown in Fig. 4(a), during t_0∼t_1, when S_1, S_4, S_6, and S_7 are turned ON, v_{AN} is equal to the voltage across the resonant capacitor C_1, which can be expressed as $v_{AN} = v_{C1}$. v_{BN} is opposite to the voltage across the resonant capacitor C_2, which can be expressed as $v_{BN} =$ -v_{C2}. Because the voltage across C_1 and C_2 are balanced, $v_{AN} = v_{C1} = v_{C2} =$ -v_{BN}. Meanwhile, v_{CO} is opposite to the voltage across the split capacitor C_4, which can be expressed as $v_{CO} =$ -v_{C4}. v_{DO} is equal to the voltage across the split capacitor C_3, which can be expressed as $v_{DO} = v_{C3}$. Because the voltage across C_3 and C_4 are balanced, $v_{CO} = v_{C3} = v_{C4} =$ -v_{DO}.

In this mode, $v_{AN} =$ -v_{BN}, $v_{CO} =$ -v_{DO}, and the directions of i_{p1} and i_{p2} are opposite, which will cancel out each other.

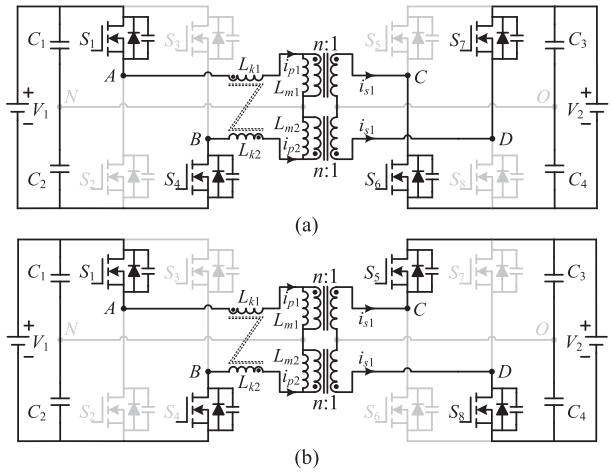

Fig. 4. Equivalent circuit of the converter in the DAB mode. (a) During $t_0 \sim t_1$. (b) During $t_1 \sim t_2$.

Then, there will be no current injected into the nodes *N* and *O*. Therefore, C_1∼C_4 will be bypassed. And there will be only leakage inductors L_{k1} and L_{k2} in the *LC* tank. In this mode, the amplitude of i_{p1} and i_{p2} are the same, but the directions of i_{p1} and i_{p2} are opposite, namely, $i_{p1} =$ -i_{p2}. Then, (1) can be rearranged as

$$\begin{cases} v_{L1} = (L_k + M)\frac{di_{p1}}{dt} \\ v_{L2} = (L_k + M)\frac{di_{p1}}{dt} \end{cases}. \tag{5}$$

Then, the equivalent inductance of the coupled inductor can be obtained from (5) and expressed as

$$L_{\text{DAB}} = L_k + M = (1 + k)L_k. \tag{6}$$

The transferred power of the converter in the DAB mode is

$$P(\varphi) = \frac{nV_1V_2\varphi(1-2\varphi)}{2L_{DAB}f_s} = \frac{nV_1V_2\varphi(1-2\varphi)}{2(1+k)L_kf_s} \tag{7}$$

where f_s is the switching frequency of the converter.

As analyzed previously, the proposed converter only needs to control the PWM signals to change the *LC* tank structure between *LLC* and DAB modes. Compared to the existing method to combine the *LLC* converter and DAB converter, the proposed method does not need to add any other switches or diodes to change the *LC* tank for the converter when operating between different modes, which eliminates the extra driver circuit for the additional switches and reduces the cost for the system. In the *LLC* mode, C_1, C_2, L_{k1}, and L_{k2} form the resonant tank. And the converter can be regarded as two parallel-connected half-bridge *LLC* converters. When C_1, C_2, C_3, and C_4 are bypassed, the converter can work in the DAB mode. Meanwhile, due to the utilization of the modulated coupled inductor, the equivalent leakage inductances in two operation modes can be exchanged between $(1 - k)L_k$ and $(1 + k)L_k$. Then, the equivalent inductance of the *LC* tank can be different for two operation modes, which can simplify the parameters design process for the converter. Consequently, the *LC* tank parameters of the two operation modes can be designed separately. The small equivalent inductance is suitable for resonance with resonant capacitors in

the *LLC* mode. And the equivalent larger inductance is adopted to transfer the power in the DAB mode. Besides, all switches of the proposed converter are operated in a high-frequency mode and used to transfer the major power.

III. Design Consideration

First, the turns ratio of the transformer is calculated as

$$n = MV_1/V_2 \tag{8}$$

where M is the voltage gain of the converter.

Second, the design of the resonant capacitance can be according to the rated power P_{rated} of the converter, which can be referred to [15] and expressed as

$$C_1 = \frac{P_{\text{rated}}}{2f_s \Delta u V_1} \tag{9}$$

where Δu is the voltage ripple of the resonant capacitor.

Third, the parameters of the coupled inductor can be designed according to the equivalent leakage inductance in two modes. When the converter operates in the *LLC* mode, the equivalent inductance of the coupled inductor can be calculated according to (4) and expressed as

$$L_{\text{LLC}} = (1-k)L_k = \frac{1}{4\pi^2 f_r^2 C_1}. \tag{10}$$

When the converter operates in the DAB mode, the equivalent inductance of the coupled inductor can be calculated according to (7) and expressed as

$$L_{\text{DAB}} = (1+k)L_k = \frac{nV_1V_2\varphi_{\max}(1-2\varphi_{\max})}{2f_s P_{\text{rated}}} \tag{11}$$

where $\varphi_{\max}$ is the phase-shift ratio when the output power is P_{rated}. From (10) and (11), the coupling coefficient and the self-inductance of the coupled inductor can be obtained.

Finally, the magnetizing inductance of the transformer can be designed to realize ZVS for the converter in the *LLC* mode, which can be calculated according to [14], and expressed as

$$L_m \le \frac{t_{\text{dead}}}{8C_j f_s} \tag{12}$$

where C_j is the total junction capacitor of the switches. And t_{dead} is the dead time of the PWM signals. Meanwhile, the magnetizing inductance is not only helpful to achieving ZVS in the *LLC* mode but also conducive to the realization of ZVS for secondary-side switches in the DAB mode.

IV. Experimental Results

In this letter, a 2000-W prototype is built to verify the effectiveness of the proposed dual-mode bidirectional *LLC*-DAB converter, which is illustrated in Fig. 5. The parameters of the converter are shown in Table I. And the parameters of the modulated coupled inductor are shown in Table II.

The steady-state waveforms of the converter with two operation modes are illustrated in Fig. 6. The waveforms in the *LLC* mode are shown in Fig. 6(a). As seen, the converter can operate with typical resonant waveforms, and the directions of i_{p1} and i_{p2} are the same. The waveforms in the DAB mode are shown in Fig. 6(b). As seen, the directions of i_{p1} and i_{p2} are opposite, which will cancel each other, leading to bypass for resonant capacitors.

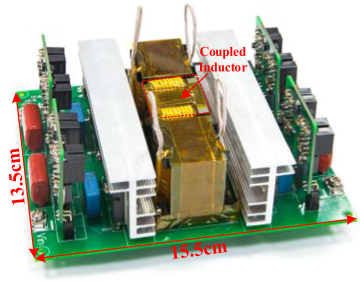

Fig. 5. Prototype of the proposed dual-mode *LLC*-DAB converter.

TABLE I
Parameters of the Prototype

Item	Value
Rated power (P_{rated})	2000 W
Primary side voltage (V_1)	400 V
Secondary side voltage (V_2)	400 V
Switching frequency (f_s)	230 *kHz*
Turns ratio of transformer (n)	20:20
Resonant capacitors (C_1 and C_2)	54 *nF*
Split capacitors (C_3 and C_4)	10 μF
Self-inductance (L_k)	12.6 μH
Mutual-inductance (M)	3.8 μH
Coupling coefficient (k)	0.3
Magnetizing inductance (L_m)	90 μH

TABLE II
Parameters of the Modulated Coupled Inductor

Item	Value
The effective core area	218 mm^2
The air gap length of the center leg	0.584 mm
The air gap length of the side legs	0.511 mm
Turns of two windings	8

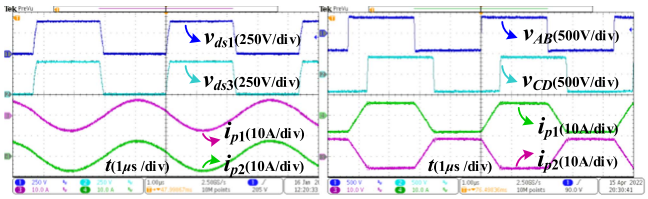

(a) (b)

Fig. 6. Comparisons of operation waveforms in different operation modes. (a) *LLC* mode. (b) DAB mode.

Fig. 7(a) shows v_{AN}, v_{BN}, v_{CO}, and v_{DO} in the *LLC* mode. As seen, the directions of v_{AN}, v_{BN}, v_{CO}, and v_{DO} are the same, leading to the resonance for L_{k1}, L_{k2}, C_1, and C_2. On the other hand, in the DAB mode, the directions of v_{AN} and v_{BN} are opposite, and the directions of v_{CO} and v_{DO} are opposite as well, which are shown in Fig. 7(b), leading to bypass for C_1, C_2, C_3, and C_4.

The ZVS waveforms of the converter are illustrated in Figs. 8 and 9. v_{gs1} and v_{gs5} are the driving signals of S_1 and S_5. v_{gs3} and v_{gs7} are the driving signals of S_3 and S_7. v_{ds1} and v_{ds5} are the drain–source voltage of S_1 and S_5. v_{ds3} and v_{ds7} are the

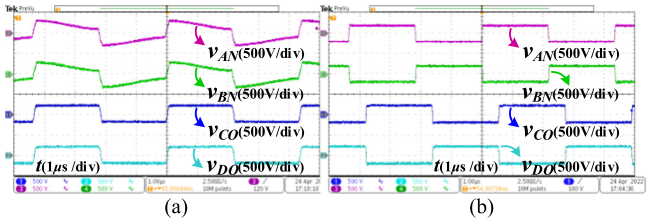

Fig. 7. v_{AN}, v_{BN}, v_{CO}, and v_{DO} in different operation modes. (a) *LLC* mode. (b) DAB mode.

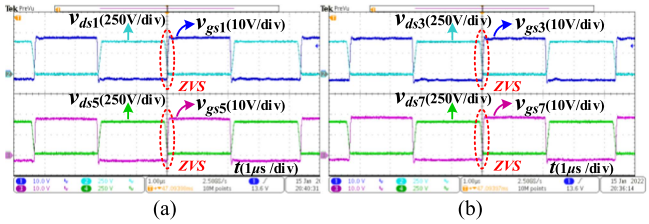

Fig. 8. ZVS waveforms in the *LLC* mode at rated power. (a) ZVS waveforms of S_1 and S_5. (b) ZVS waveforms of S_3 and S_7.

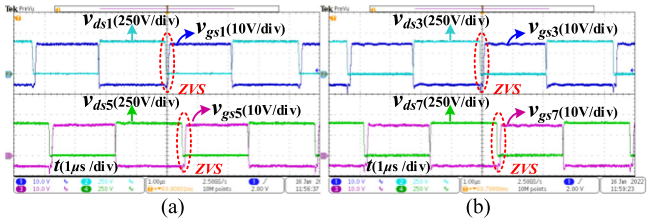

Fig. 9. ZVS waveforms in the DAB mode at rated power. (a) ZVS waveforms of S_1 and S_5. (b) ZVS waveforms of S_3 and S_7.

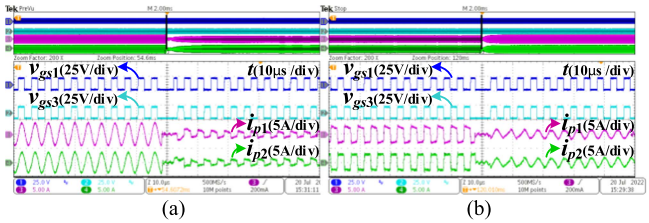

Fig. 10. Mode transition waveforms. (a) *LLC* mode switches to DAB mode. (b) DAB mode switches to *LLC* mode.

drain–source voltage of S_3 and S_7. As seen, all switches can achieve ZVS for two operation modes at rated power.

Fig. 10 shows the transition waveforms when the converter switches between the *LLC* mode and the DAB mode. As seen, the PWM signals are changed when the operation modes need to be switched. To avoid the inrush current in the transition process, low-level driving signals of one switching period are inserted between two operation modes. It can be seen that there is no current overshoot for the modulated coupled inductor current in the transition process between the two operation modes.

Fig. 11 shows the comparison of output voltage and efficiency between the two modes. As seen, when the proposed converter operates in the *LLC* mode, it has a higher conversion efficiency, but the output voltage is unregulated. On the other hand, the output voltage in the DAB mode is tightly regulated. However,

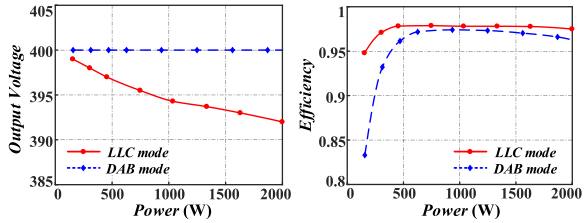

Fig. 11. Comparison of output voltage and efficiency between two modes. (a) Output voltages. (b) Conversion efficiency.

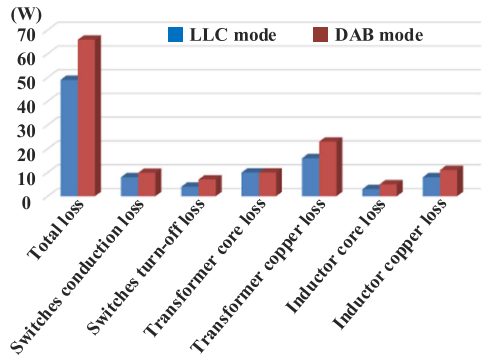

Fig. 12. Loss breakdown of the converter operated in two modes at rated power.

the efficiency in the DAB mode is slightly lower than that in the *LLC* mode.

The loss breakdown of the converter operating in two modes is illustrated in Fig. 12. As seen, the total loss of the converter in the DAB mode is higher than that in the *LLC* mode. Because the rms current in the DAB mode is larger than that in the *LLC* mode, the conduction loss in the DAB mode (including the switches conduction loss, transformer copper loss, and inductor copper loss) is larger than that in the *LLC* mode. Meanwhile, the switches turn-OFF loss in the DAB mode is larger than that in the *LLC* mode, because the turn-OFF current in the DAB mode is larger than that in the *LLC* mode. For the core loss of the modulated coupled inductor, because the flux will be canceled in the center leg of the EI core in the *LLC* mode, the core loss in the *LLC* mode is smaller than that in the DAB mode.

V. Conclusion

This letter proposes a dual-mode bidirectional *LLC*-DAB converter to combine the *LLC* converter and DAB converter. By modulating the PWM signals, the operation mode can be exchanged between *LLC* mode and DAB mode through changing the *LC* tank structure without adding any other additional diodes or switches. Meanwhile, by utilizing the modulated coupled inductor, the *LC* tank parameters of the two operation modes are different. The smaller inductance is used to resonate with resonant capacitors in *LLC* mode, and the larger inductance is adopted to transfer the power in the DAB mode, leading to a separate design of the *LC* tank for the two operation modes. Through analysis of the experimental results, it can be obtained that both two operation mode have their respective advantages.

The higher efficiency in the *LLC* mode, but the unregulated output voltages. The tight voltage regulation for DAB mode, but lower efficiency. Therefore, the proposed converter can exchange the operation modes according to the corresponding operating conditions.

REFERENCES

[1] B. Zhao, Q. Song, W. Liu, and Y. Sun, "Overview of dual-active-bridge isolated bidirectional DC–DC converter for high-frequency-link power-conversion system," *IEEE Trans. Power Electron.*, vol. 29, no. 8, pp. 4091–4106, Aug. 2014, doi: 10.1109/TPEL.2013.2289913.

[2] Y. Liao et al., "Single-stage DAB-LLC hybrid bidirectional converter with tight voltage regulation under DCX operation," *IEEE Trans. Ind. Electron.*, vol. 68, no. 1, pp. 293–303, Jan. 2021, doi: 10.1109/TIE.2020.2965495.

[3] T. Jiang, J. Zhang, X. Wu, K. Sheng, and Y. Wang, "A bidirectional LLC resonant converter with automatic forward and backward mode transition," *IEEE Trans. Power Electron.*, vol. 30, no. 2, pp. 757–770, Feb. 2015, doi: 10.1109/TPEL.2014.2307329.

[4] H. Li, Z. Zhang, S. Wang, J. Tang, X. Ren, and Q. Chen, "A 300-kHz 6.6-kW SiC bidirectional LLC onboard charger," *IEEE Trans. Ind. Electron.*, vol. 67, no. 2, pp. 1435–1445, Feb. 2020, doi: 10.1109/TIE.2019.2910048.

[5] D. Sha, J. Zhang, and K. Liu, "Leakage inductor current peak optimization for dual-transformer current-fed dual active bridge DC–DC converter with wide input and output voltage range," *IEEE Trans. Power Electron.*, vol. 35, no. 6, pp. 6012–6024, Jun. 2020, doi: 10.1109/TPEL.2019.2952650.

[6] B. Zhao, Q. Song, and W. Liu, "Power characterization of isolated bidirectional dual-active-bridge DC–DC converter with dual-phase-shift control," *IEEE Trans. Power Electron.*, vol. 27, no. 9, pp. 4172–4176, Sep. 2012, doi: 10.1109/TPEL.2012.2189586.

[7] S. Mukherjee, A. Kumar, and S. Chakraborty, "Comparison of DAB and LLC DC–DC converters in high-step-down fixed-conversion-ratio (DCX) applications," *IEEE Trans. Power Electron.*, vol. 36, no. 4, pp. 4383–4398, Apr. 2021, doi: 10.1109/TPEL.2020.3019796.

[8] C. Sun, X. Zhang, J. Zhang, M. Zhu, and J. Huang, "Hybrid input-series–output-series modular DC–DC converter constituted by resonant and nonresonant dual active bridge modules," *IEEE Trans. Ind. Electron.*, vol. 69, no. 1, pp. 1062–1069, Jan. 2022, doi: 10.1109/TIE.2021.3055175.

[9] N. D. Dao, D. Lee, and Q. D. Phan, "High-efficiency SiC-based isolated three-port DC/DC converters for hybrid charging stations," *IEEE Trans. Power Electron.*, vol. 35, no. 10, pp. 10455–10465, Oct. 2020, doi: 10.1109/TPEL.2020.2975124.

[10] L. Wang, Q. Zhu, W. Yu, and A. Q. Huang, "A medium-voltage medium-frequency isolated DC–DC converter based on 15-kV SiC MOSFETs," *IEEE J. Emerg. Sel. Topics Power Electron.*, vol. 5, no. 1, pp. 100–109, Mar. 2017, doi: 10.1109/JESTPE.2016.2639381.

[11] J. Wu, S. Li, S.-C. Tan, and S. Y. R. Hui, "Capacitor-clamped LLC resonant converter operating in capacitive region for high-power-density EV charger," *IEEE Trans. Power Electron.*, vol. 36, no. 10, pp. 11456–11468, Oct. 2021, doi: 10.1109/TPEL.2021.3068693.

[12] Y. P. Chan, C. S. Wong, and K. H. Loo, "Dual-mode modulation scheme with seamless transition for a tunable immittance-based DAB converter featuring high-efficiency performance over whole output power range," *IEEE Trans. Power Electron.*, vol. 35, no. 9, pp. 9184–9201, Sep. 2020, doi: 10.1109/TPEL.2020.2971106.

[13] X. Chen, G. Xu, H. Han, Y. Sun, Y. Liu, and M. Su, "Modulated coupled inductor for input-serial–output-parallel dual-active-bridge converter," *IEEE Trans. Ind. Electron.*, vol. 69, no. 6, pp. 6450–6455, Jun. 2022, doi: 10.1109/TIE.2021.3088364.

[14] B. Lu, W. Liu, Y. Liang, F. C. Lee, and J. D. van Wyk, "Optimal design methodology for LLC resonant converter," in *Proc. IEEE 21st Annu. Appl. Power Electron. Conf. Expo.*, 2006, pp. 533–538, doi: 10.1109/APEC.2006.1620590.

[15] G. Xu, J. Huang, H. Dan, M. Su, and R. Zou, "A bidirectional symmetrical C4LC-DCX resonant converter with power limitation capability," *IEEE J. Emerg. Sel. Topics Power Electron.*, vol. 10, no. 1, pp. 868–880, Feb. 2022, doi: 10.1109/JESTPE.2021.3099476.